A Localization Method for Wireless Capsule Endoscopy Using Side Wall Cameras and IMU Sensor

seyed shahim vedaei (shahim.vedaei@usask.ca)
University of Saskatchewan
khan wahid
University of Saskatchewan

Research Article

Keywords: mono-chromatic cameras, installed along the wide wall, other methods

Posted Date: January 6th, 2021

DOI: https://doi.org/10.21203/rs.3.rs-137277/v1

A Localization Method for Wireless Capsule Endoscopy Using Side Wall Cameras and IMU Sensor

Seyed Shahim Vedaei[1, *], **and Khan Wahid**[2]

[1]PhD. student, Department of Electrical Engineering, University of Saskatchewan, SK, S7H 5A9, Canada.
[2]Faculty of Electrical Engineering, University of Saskatchewan, SK, S7H 5A9, Canada.
[*]shahim.vedaei@usask.ca

ABSTRACT

Localizing the endoscopy capsule inside gastrointestinal (GI) system provides key information which leads to GI abnormality tracking and precision medical delivery. In this paper, we have proposed a new method to localize the capsule inside human GI track. We propose to equip the capsule with four side wall cameras and an Inertial Measurement Unit (IMU), that consists of 9 Degree-Of-Freedom (DOF) including a gyroscope, an accelerometer and a magnetometer to monitor the capsule's orientation and direction of travel. The low resolution mono-chromatic cameras, installed along the wide wall, are responsible to measure the actual capsule movement, not the involuntary motion of the small intestine. Finally, a fusion algorithm is used to combine all data to derive the traveled path and plot the trajectory. Compared to other methods, the presented system is resistive to surrounding conditions, such as GI nonhomogeneous structure and involuntary small bowel movements. In addition, it does not require external antenna or arrays. Therefore, GI tracking can be achieved without disturbing patients' daily activities.

Introduction

Invention of Wireless Capsule Endoscopy (WCE) was a breakthrough in diagnosing gastrointestinal (GI) problems. WCE is designed in a small size electronic device that the patient can swallow, and it then travels through the GI tract. A camera is placed on top of the capsule[1], and continuously captures images and transmits them to a data logger outside of the body. Physicians then examine the images to detect any abnormalities. In another type of WCE, camera is replaced with sensors such as temperature, pressure, Potential of Hydrogen (pH)[2] or light spectrum analyser sensors[3,4]. WCE could pinpoint the abnormalities in GI system. Image processing algorithms detect diseases and notify the doctors for further examination[5]. However, doctors are interested in images which are tagged by their location with respect to the GI pathway, so that they could examine the disease progression and treat accordingly.

The topic of localizing the capsule inside GI has gained a lot of interests among researchers. Many attempts have been done till now. In a broader view, the position could be defined with respect to either GI track anatomy, or external reference point, such as an antenna. In most cases, electronic capsules equipped with transmitting modules which transfer data through Radio frequency (RF) signals. Hence, RF localization techniques are promising options. Nafchi *et al.*[6] have utilized Directional of Arrival (DoA) and Time of Arrival (ToA) techniques in conjunction with Inertial Measurement Unit (IMU) sensor to locate the capsule. An arrangement of circular antennas array around the body receives the signals and measures the distance. Simultaneously, they are able to estimate the position and velocity of the capsule with the help of the IMU sensor. Non-homogenous environment inside the body leads to fluctuation of received signals, so they have used an extended Kalman filter to moderate the instabilities of signals. Their proposed method results up to 10 mm error in tracking the capsule position. Ting-Goh[7] presents an integrated tracking method of DoA and IMU measurements. A combination of 8 columns of array antennas outside of the body capture signals and measure the distance toward the capsule. In addition, an IMU sensor determine the heading direction, then Unscented Kalman Filter fuses all data to provide the capsule's location in Three Dimensional (3D) space. Some articles used the Received Signal Strength Indicator (RSSI)[8,9,10] to measure the signal level and anatomize the body with pre-defined propagation properties. Later, they extracted [8] the 3D position with average and maximum positional error of 37.7 mm and 114 mm, respectively. The accuracy is not enough to be considered as a general solution; technical problem such as line-of-sight put these methods into a challenge. On top of that, in practical experiments, the antennas are mounted on patient's body which used as a reference for localization, while the reference body is also in motion.

Some works have focused on other external localization techniques based on magnetic field. The idea is to integrate a small magnet inside the capsule, then an external magnetometer will measure the magnetic field[11]; finally, methods such as triangulation locate the capsule in 3D space. The main advantage of these approaches over other localization methodologies

is that low-frequency magnetic signals can pass through the human tissues without degradation, and it is an advantage over RF approaches which are depending on the RF signal's strength. Another advantage is that, the magnetic sensors do not need the line-of-sight vision to detect the capsule. All in all, the computational complexity and overall accuracy of magnetic-based techniques are comparative to RF localization methods. Taddese and *et al.*[12] make use of magnetic-based localization on their paper and achieved position and orientation accuracies lower than 5 mm and 6°, respectively. A recent study by Shao *et al.*[13], they have enclosed a magnet with bio-tissue and tried to localize it. They showed that the non-ferromagnetic bio-tissue has minor effect on the magnetic fields, so positioning accuracy will not be influenced by human tissues. In addition, their proposed method obtains the initial guess of position through the variance-based algorithm which leads to reduce the iterations and achieve higher localization accuracy. Shao reported the positioning error up to 10 mm and average orientation error of 12°. External positioning also is facing significant challenges, such as interference between multiple magnetic sources and uncertain initial guess for optimization algorithm which leads to drift in estimating the location. Moreover, the need for fixed position external reference is also limiting the application of magnetic localization methods for clinical and experimental usage

Internal localization could be performed via image processing techniques. Lee and his colleagues[23] have equipped a traditional endoscopy system with an IMU sensor to get the camera's heading in order to compensate the rotation. Lee's system gives the rotation angles; however, the position is still unknown. Turan *et al.*[17] have proposed a monocular visual odometry for WCE. Utilizing the advantage of deep Recurrent Convolutional Neural Networks (RCNNs), the system is trained in an end-to-end manner, so there is no need to fine-tune the network parameters. Similar to previous methods, image processing localization algorithms encounter with some critical issues, such as inappropriate accuracy due the lack of reference point inside the body. Considering occasional movements inside the body and limited number of frames captured and transmitted by the WCE, it will increase the positioning error.

Some other types of localization methods are also available, for example, Kalantar-Zadeh *et al.*[24] developed an electronic capsule, capable of sensing various gases in the gut. This capsule can sense oxygen, hydrogen, and carbon dioxide. They performed a human pilot trial and sensed gas concentration profile with respect to GI organs. Their research showed that, carbon dioxide concentration profile is a promising option to localize the capsule inside the body. In a recent article by Jang and his colleges[25], an endoscopy capsule has been developed with two cameras located at capsule's sides and it paves the path for taking pictures of the internal GI's walls. Their system has the ability to localize the capsule inside the GI by RSSI technique. They have claimed an average localization error of 1 cm.

Medical and radiological imaging, such as Magnetic Resonance Imaging (MRI), Computerized Tomography (CT), ultrasound, X-ray, and gamma ray techniques or hybrid methods are also considered for capsule localization. But they are not easily combined with WCE because of the necessity for continuous imaging over all examination process which may long as 8 hours.

Above all, most localization techniques suffer from non-predictable involuntary movement of the small bowel itself, which disrupts the relative movement between the human body and the sensor array. For example, the body may move according to an external coordinates system, while the GI organ itself may move or rotate within the body coordinates in a different direction. As of today, no method is able to address this problem. In the next section, we propose a new approach for WCE localization that addresses this unique issue and results in a better accuracy.

Methods

Human GI tract is a tubular pathway, using this feature we have developed a device for WCE localization. To shed some light on the method, we started this section by an example. Thinking of a Metro which is travelling in a tunnel, a man in the wagon has a compass in his hand and he is looking toward the tunnel's wall. The compass gives the wagon's heading direction, in addition, that person by looking toward the tunnel's wall knows how far it has traveled. Similarly, we have proposed a system that is composed of an IMU sensors, side wall motion cameras, processing unit and transceiver unit. The orientation of the device comes from an IMU sensor and capsule's displacement derives from side wall cameras. On top of that, a fusion algorithm is introduced to combine the orientation data and the displacement. Finally, the system is able to plot the traveled trajectory in a 3D space.

Capsule prototype

In this section an overview of the proposed device and necessary modules and components is provided. The system block diagram is shown on Figure 1. The processing unit is a bridge between different parts of the system, and it controls all modules including IMU sensor, side wall motion cameras and RF transceiver unit. The capsule is equipped with four cameras, one for each side; however, to make it easy for presentation, only two of them is depicted in the schematic. The final prototype is shown in Figure 2(a) & (b). The capsule size is 3.5 cm × 3.5 cm × 4 cm. Different parts of the capsule prototype are shown in

Figure 2(c). The capsule is responsible to capture the data and sends them in a raw format to the data-logger outside of the body; therefore, the capsule does not require any data processing which significantly reduces the design complexity. After receiving the data, a computer-based program is responsible to apply algorithms and calculate the 3D result.

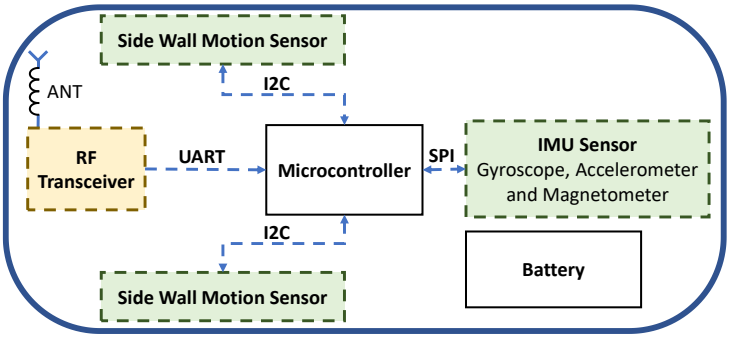

Figure 1. Schematic overview of the capsule.

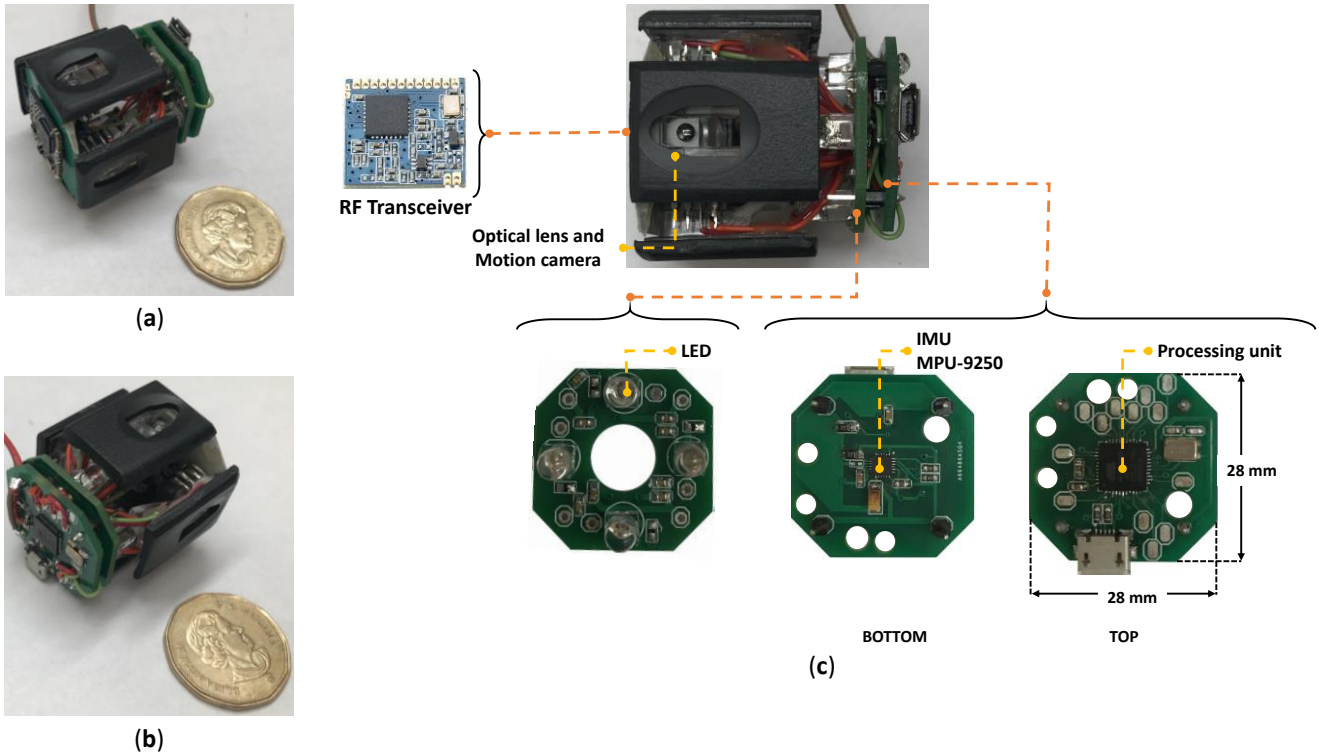

Figure 2. (**a**) & (**b**) Capsule prototype designed in the lab (**c**) Various parts of the lab prototype.

Processing unit

A microcontroller (µC) is responsible to connect all components together to work as a system. Individual sensors are connected to the µC through specific protocols. For this project we have used ATmega32U4 as a processing unit, this µC has built-in I^2C and Serial Peripheral Interface (SPI) which make it simpler to use for different applications.

The µC reads all sensors then sends the raw data using a wireless link. The capsule reads 2 Bytes from each motion camera. Considering four side wall motion cameras, the µC reads 8 Bytes in total. The IMU sensor produces 18 Bytes. Finally, the µC creates a frame of 28 Bytes with all data and necessary headers, then sends it to a data-logger outside of the body. In order to reduce the transmission power, the µC only sends the frame when it detects a motion.

Side wall motion camera

Visual odometry is a technology which measures the displacement using optical properties of the scene. In principle, a camera captures the pictures and sends the frames out of the body for processing, then an image processing algorithm calculates the displacement. However, adding 4 cameras on capsule's side and sending frames need huge power resources and transmission band width. While, processing images inside the capsule adds complexity to the design.

Motion measurement camera is an Integrated Circuit (IC) that has a low-resolution camera with on-board Digital Signal Processing (DSP) unit to run the image processing algorithms and communication interface, all on a small silicon dye. Figure 3 illustrates the motion camera, the actual size of this IC is 1 mm × 2 mm. and Figure 3(c) shows a closer look at which the light sensitive part is a Charged Coupled Device (CCD) camera that has 18×18 pixels sensor array. For our design the selected chip with part number YS8008B is selected. This IC works with 3 V power supply and it has Inter-Integrated Circuit (I^2C) interface protocol.

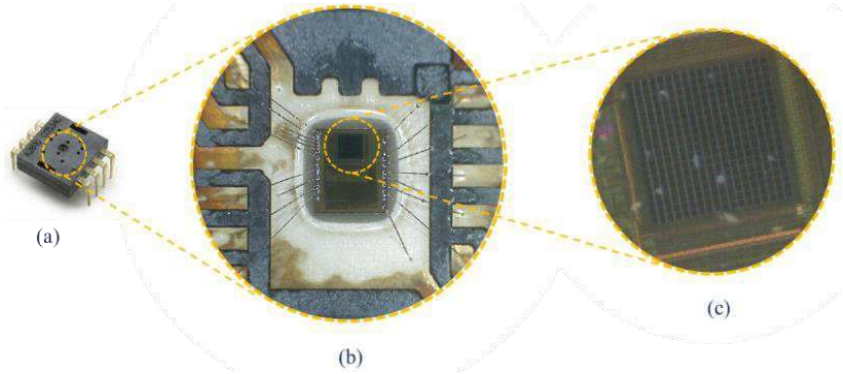

Figure 3. Optical motion measurement sensor (similar to the one used in computer optical mouse today), (**a**) Dual inline package IC, (**b**) Microscopic view and (**c**) 18×18 pixels CMOS camera.

Side wall motion camera consists of three basic components: motion sensor (monochromatic camera), optical lens and lighting source. Figure 4(a) illustrates the camera and related optical system. The optical system consists of two parts, a prism and a focus lens. The prism guides the light source so that it lights up the camera view then the lens focuses the reflected light from surface to the CCD. The light guider is positioned so that it could receive the light rays from the right side and guides the rays with correct angle to be emitted to the surface and reflected precisely to the CCD. In addition, a Light Emitting Diode (LED) with red color is selected to have the highest reflection rate in the GI.

Figure 4(b) shows how the motion estimation algorithm is working. h is the fixed distance between the camera and intestine's wall. θ is the angular position of each pixel, and $\vec{D}$ is a vector that shows the displacement of individual pixels compared to the previous frame. The displacement comes from four cameras which are located at the capsule's side wall. As a rule of thumb at least one camera should stick to the intestine's wall. The camera takes pictures every 10 ms. Then, pictures are compared and distinct points at each frame will be selected. Then, the algorithm looks for the same point at adjacent frames. The algorithm is able to calculate motion vectors for individual pixels ($\vec{D}_1, \vec{D}_2$, ...). Finally, it computes the average vector and finds the average displacement vector ($\vec{D}_m$).

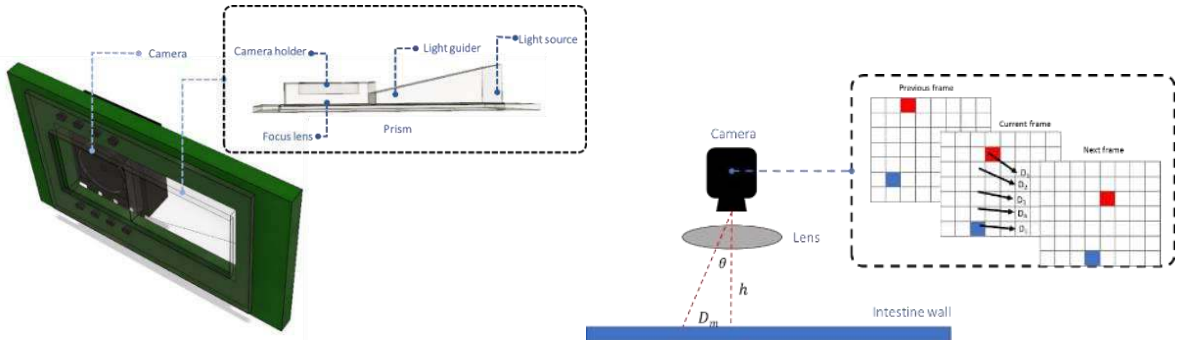

(**a**) (**b**)

Figure 4. (**a**) Side wall camera and its optical parts, (**b**) motion vector calculation.

Inertial Measurement Unit

An Inertial Measurement Unit, commonly known as an IMU, is an electronic device that measures and reports orientation, velocity, and gravitational forces using accelerometers and gyroscopes and often magnetometers. For this project we have used an IMU sensor MPU9250 with size of less than 5 mm × 5 mm.

Gyroscope measures angular velocity, in other words gyroscope reports how fast the device is spinning about an axis. Rotation about different axes is illustrated in Figure 5, which named as roll, pitch and yaw. The gyroscope gives the rate of change of the angular position over time with a unit of $\left(\frac{\text{deg}}{\text{s}}\right)$, according to equation 1.

$$\dot{\theta} = \frac{d\theta}{dt} \qquad (1)$$

In order to derive angular position, we integrate the angular velocity in a period of time, it can be mathematically shown as equation 2.

$$\theta(t) = \int_0^t \dot{\theta}(t)\, dt \approx \sum_0^t \dot{\theta}(t) T_s \qquad (2)$$

where, T_s is the sampling time and it represents the time interval between samples. The gyroscope data is reliable only on the short term, as it starts to drift on the long term. Hence, accelerometer data is used to compensate the gyroscope data.
The accelerometer measures all forces that are working on the object and sends them as A_x, A_y and A_z. To obtain the angular position with the accelerometer, we are going to determine the position of the earth gravity vector which is always visible on the accelerometer. This can be done by using an atan function. In addition, the yaw derived from magnetometer; so, a fusing algorithm is required to combine the sensors all together.

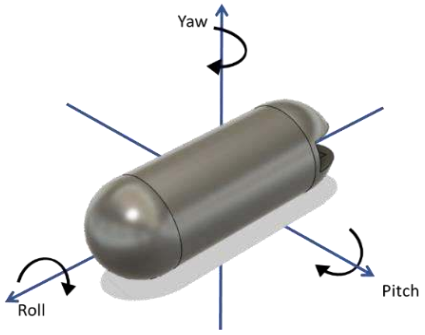

Figure 5. rotation about different axes.

The IMU sensor must be calibrated before use to compensate the surrounding conditions and noises. In order to produce an accurate orientation estimation, the magnetometer should see the earth's magnetic field, and any ignore conditions that affect the earth's magnetic properties. The magnetic measurements will be subjected to two types of distortion - hard iron and soft iron distortions. Objects that produce a magnetic field cause the hard iron distortion, which is a permanent bias in magnetometer output. Soft iron distortion, on the other hand, caused by the ferromagnetic objects, and leads to deflections or alterations in the existing magnetic field. In order to cancel hard iron effect bias terms should be added to the raw data,

meanwhile, correction factors in matrix format will multiply to the measured magnetic field to neutralize the soft iron distortion according to equation 3.

$$\begin{bmatrix} M_{xc} \\ M_{yc} \\ M_{zc} \end{bmatrix} = \begin{bmatrix} S_{11} & S_{12} & S_{13} \\ S_{21} & S_{22} & S_{23} \\ S_{31} & S_{32} & S_{33} \end{bmatrix} \times \begin{bmatrix} M_x \\ M_y \\ M_z \end{bmatrix} + \begin{bmatrix} B_x \\ B_y \\ B_z \end{bmatrix} \quad (3)$$

where, M_x, M_y and M_z are magnetic fields read from the sensor. M_{xc}, M_{yc} and M_{zc} are calibrated magnetic fields. B_x, B_y and B_z are the applied biases to compensate the hard iron effect, and S_{mn} are correction factors to remove the soft iron distortion.

Transceiver

At this stage of designing we are not concerned about modules' size, so we have hired a Lora RF module operating at 433 MHz. The Lora is configured on Transmitter/Receiver (TX/RX) mode, which is perform as serial wireless bridge, the µC sends and receive data through Universal Asynchronous Receiver-Transmitter (UART) protocol connecting to TX/RX pins via Lora.

Sensor fusion algorithm

Generally, in order to get 3D orientation of the capsule, we have to fuse all three sensors of accelerometer, gyroscope and magnetometer. Kalman filters have been demonstrating its usefulness in various applications, it not only works well in practice, but is theoretically attractive because it can be shown that of all possible filters, it is the one that minimizes the variance of the estimation error. Kalman filtering is an algorithm that provides estimates of some unknown variables given the measurements observed over time. Figure 6(a) demonstrates the IMU sensor fusing schematic. Figure 6(b) shows the 3D orientation result. The output provides an accurate orientation estimation. The fusing algorithm named Attitude and Heading Reference System (AHRS).

The next step toward capsule localization is fusing the orientation with displacement data. The capsule's orientation is derived via AHRS algorithm; and the heading vector can be calculated using roll, pitch and yaw angles according to equation 4. The heading vector should be normalized for further processing. By moving along the heading vector, we could compute the location in 3D space.

$$\begin{aligned} \vec{V}_{heading} = (-\cos(\psi)\sin(\varphi)\sin(\theta) - \sin(\psi)\cos(\theta))\hat{X} \\ +(-\sin(\psi)\sin(\varphi)\sin(\theta) + \cos(\psi)\cos(\theta))\hat{Y} \\ +(cos(\varphi)sin(\theta))\hat{Z} \quad (4) \end{aligned}$$

where, ψ is yaw, φ pitch and θ roll angles. The $\hat{X}, \hat{Y}$ and $\hat{Z}$ are the unit vectors in Cartesian coordinate system.

The motion camera sensor provides the displacement along the heading vector, then multiplying the displacement to heading vector represents the 3D projection of the capsule's movement. This is shown in equation 5.

$$\vec{D} = D_{mx}.\vec{V}_{heading} \quad (5)$$

where, $\vec{D}$ shows the 3D displacement vector, and D_{mx} is the $\hat{X}$ component of the $\vec{D}_m$. Finally, to get the 3D position, we have used the following equation:

$$P_{n+1}(x, y, z) = P_n(x, y, z) + \vec{D} \quad (6)$$

where, P_{n+1} is the new position and P_n is the previous position. Thus, we are able to calculate the new position of the capsule from the previous position. Finally, a 3D trajectory is generated.

Results and discussion

Surface patterns

In order to evaluate the motion sensor's performance, basic patterns were introduced as depicted in Figure 7(a). Patterns are expanded on horizontal columns and printed on white paper, the reflectance properties of substrate are also important, to be clarified, these patterns were printed using a black & white laser-jet printer on normal A4 paper. We put the motion sensor on top of that line and move the sensor forward, a ruler is placed to be considered as ground truth. Motion sensor moves from point 0 to 20 cm, and capture the dx displacement from the sensor, this process repeated 5 times for each pattern. The experiment has two outcomes. First of all, YS8008B could measure the displacement in all patterns except two of the parallel patterns. Sensor's sensitivity and lens' focal length are important properties for correctly capturing and analyzing the surface. Hence, several experiments are performed to evaluate the functionality of side wall motion cameras.

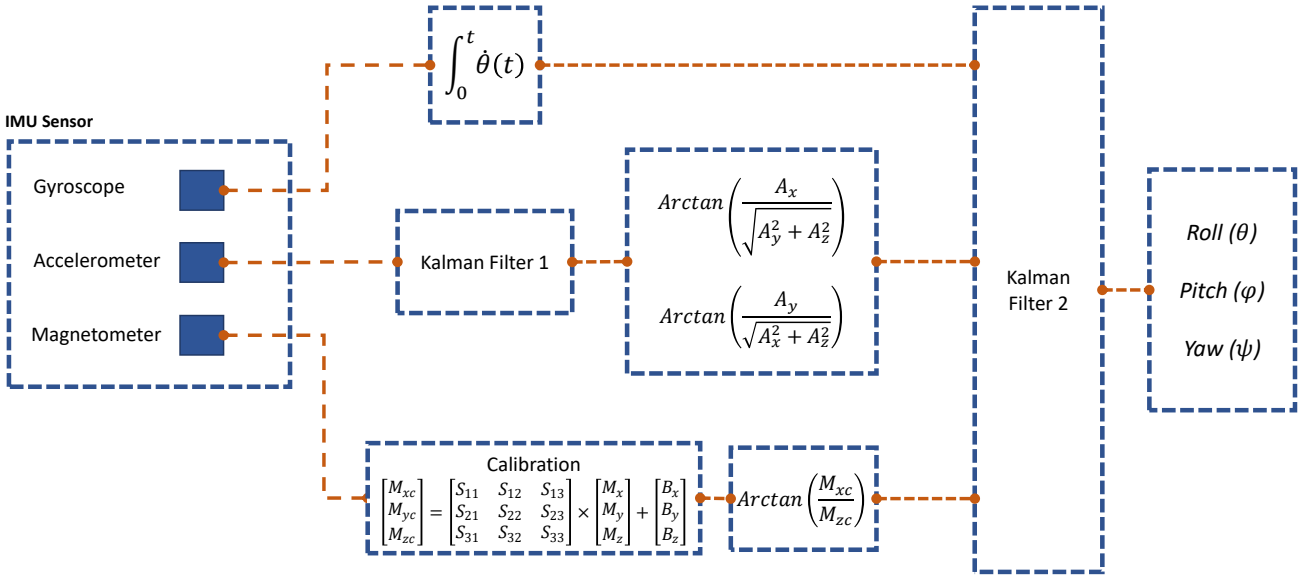

(a)

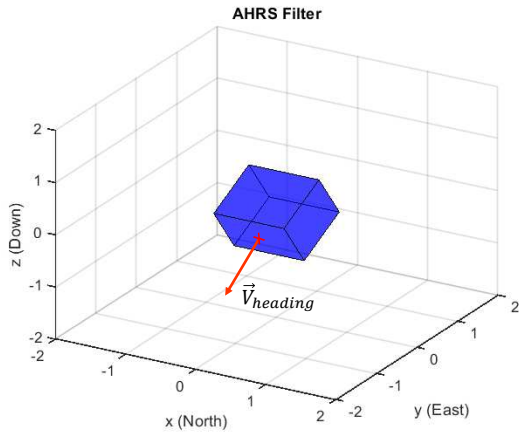

(b)

Figure 6. (**a**) IMU sensor fusing schematic, (**b**) 3D orientation result.

Optical properties of the surface are also important and should be considered. The pictures of small intestine derived from WCE are stretched and printed on paper as shown in Figure 7(b). In this way, we make sure that motion sensor will work on small intestine's texture, as well.

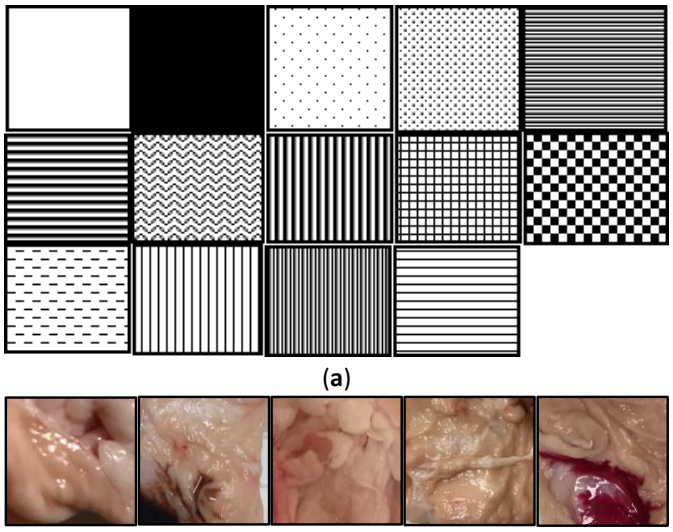

Figure 7. (**a**) Basic patterns, (**b**) colored patterns.

Surface material

In addition to that, the surface's material defines the optical reflection properties of the surface, several surface materials are selected to evaluate the performance of the motion sensor as shown in Table 1.

Surface	Perform	Detail
Aluminum foil	No	But PAW3515 motion sensor works perfectly on this surface.
Glass	No	
Mirror	No	
Transparent plastic bag	YES	Depend on beneath surface
Colored plastic bag	YES	Mostly depend on the reflection properties of the surface
Human outer skin	YES	PAW3515 does not work
Color printed image	YES	
Curved surface	YES	As long as the optical lens matches to the surface
Pig's intestine	YES	
Grounded meat	YES	Grounded meat shielded by thin plastic wrapper
Beef meat	YES	
Chicken meat	YES	

Table 1. YS8008B optical sensor movement performance on different surfaces.

By considering a curved surface, the Motion sensor works as long as the surface stick to the motion sensor's focal length. Elastic properties of the intestine help the surface keep at the right distance from the lens. The lens and CCD designed for YS8008B motion sensor work better in different focal length compare to other sensor and make YS8008B a suitable choice for our application.

1D tracking

Figure 8 illustrates another experiment to evaluate the motion sensors' accuracy. In this experiment, the capsule travels three straight line path with size of 15, 30 and 60 cm. Each experiment repeated 3 times. Figure 8(a) shows the experiment results and Figure 8(b) illustrates the error in estimating the distance. It is shown that the maximum error of ±3.71 % can be achieved in 60 cm path.

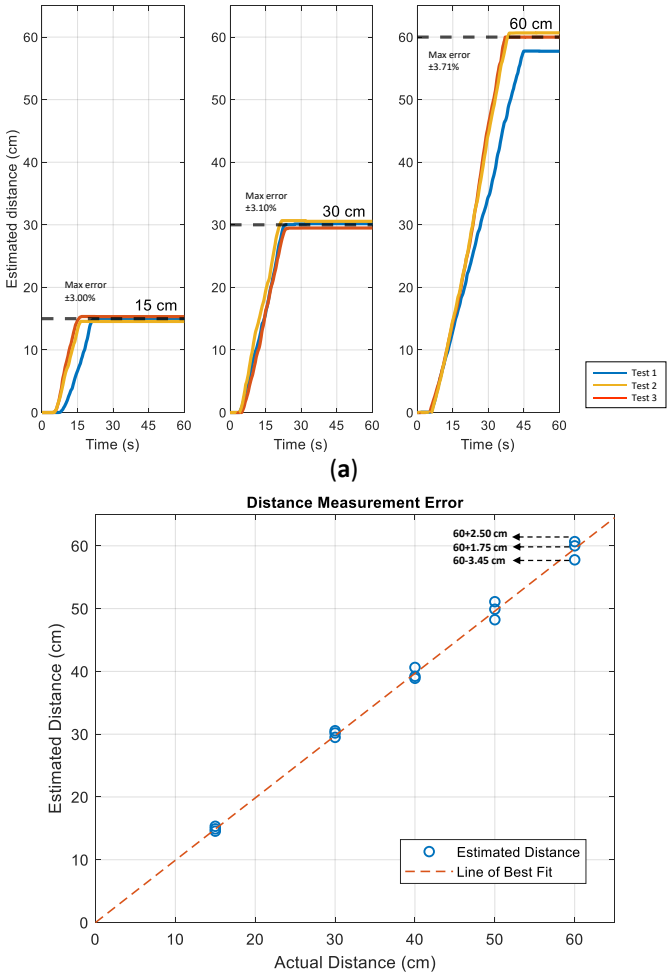

Figure 8. (**a**) Repeat the same path (**b**) Distance measurement error.

Leap and peristalsis motions

The next experiment is designed to find the maximum speed measured by motion sensor, two types of motion is considered in this part, moving at constant speed and leap motion. The YS8008B measures the displacement between two sampling time (T_s) then sends the information to the host, hence, T_s limits the maximum speeds. Shorter T_s tends to overflow the buffer, so, the error rises in displacement measurement, on the other side, longer T_s results higher drift error. In this experiment, the capsule pushed by 10 sequential jumps in $\hat{X}$ direction to reach the final point. Leap motion; the jump or sudden movement should not exceed the upper speed limit. According to our experiment ,10 ms T_s would be the optimum time, in this regard, the motion sensor would capture movements as fast as 2 cm/s.

In another experiment, the peristalsis motion is investigated. Peristalsis motion is an involuntary contraction and relaxation of muscles which leads to push food ahead of the wave. Muscle's contraction behind the food to keep it from moving backward, then longitudinal contraction to push it forward. Commonly, peristaltic waves exist in the small intestine at irregular intervals and travel for different distances, some ways travel only a few inches, others travel longer. Tracking an object which is under peristalsis motion could be difficult, due to the fact that the object might go forward and slightly backward. Figure 9(a) shows how peristalsis motion is working, due to the contraction of muscles, we could ensure that side wall cameras will stick to the GI wall. An experiment has performed in Two Dimensional (2D) tracking to monitor the side wall camera behaviors' in such movement, as well.

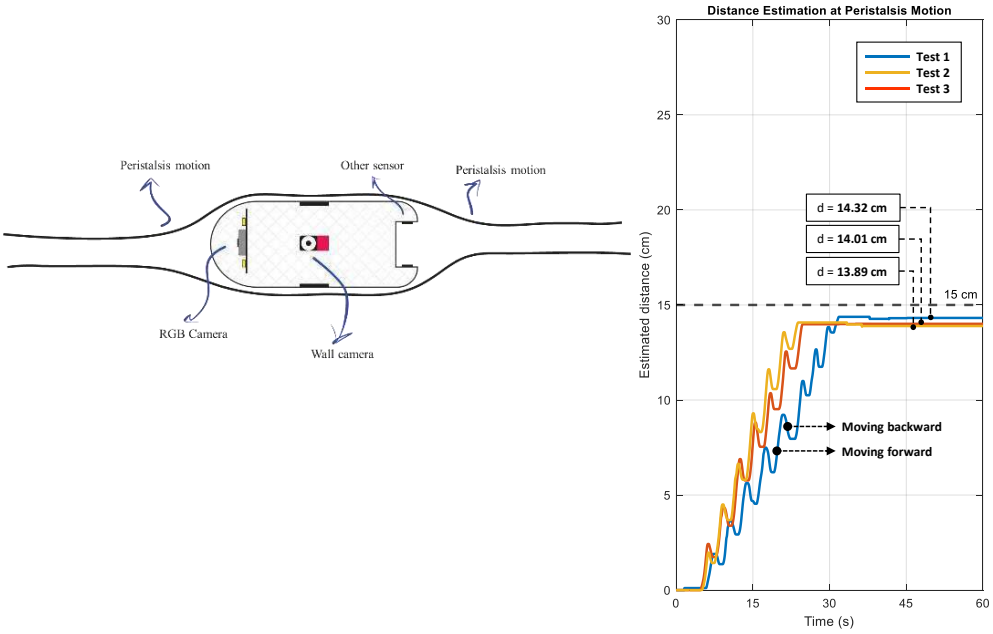

(**a**) (**b**)

Figure 9. (**a**) Peristalsis motion (**b**) experiment results.

Figure 9(b) illustrates the effect of peristalsis motion in the experiment. The capsule is traveled a 15 cm path and during the path, it moves forward and backward several times. The results show that under this condition, the error in estimated distance is around 7.4%.

2D tracking

The motion sensors have the capability to measure the displacement in both *x* and *y* directions. In 2D mode, motion sensor measures the *x* and *y* vectors, where the IMU is not used. 2D motions was performed by hand with 3 degree of freedom, the test platform is a printed path with dashed lined as reference track. The motion sensor sends *dx* and *dy*, and the algorithm integrates the data to plot the 2D trajectory. The arm moves the capsule on different trajectories as shown on Figure 10(a) and (b). The arm motions, known as ground truth, which are plotted by bashed line; the blue line is the displacement measured by motion sensor. As plots could testify, the estimated motions are not completely match with the ground truth. A maximum error of 2 cm is observed. As a result, drift error will add to the estimated distance.

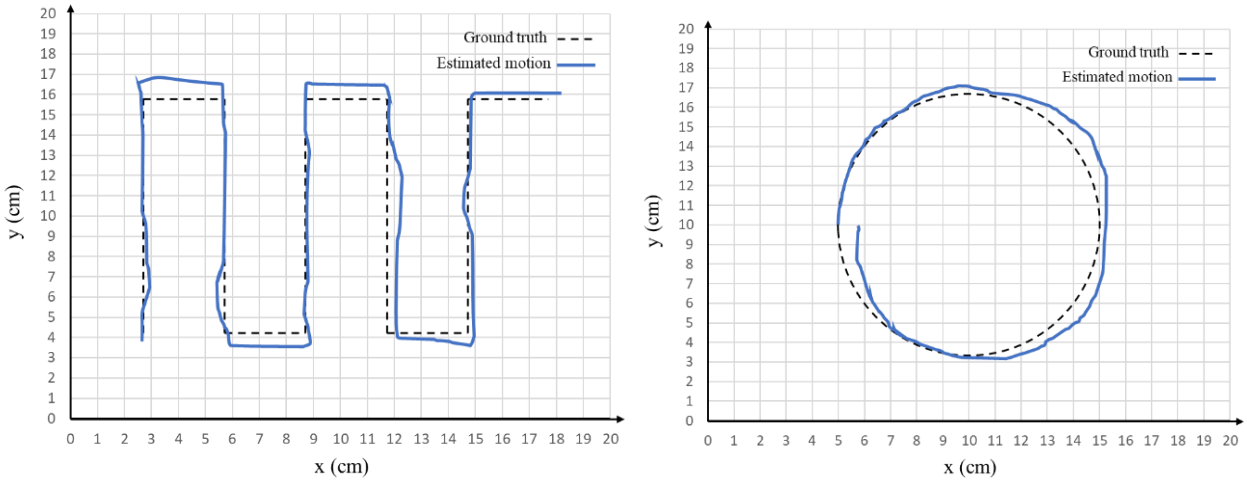

(**a**) (**b**)

Figure 10. 2D motion tracking, (**a**) & (**b**) test trajectories.

3D tracking

The actual mode of operation on capsule is the 3D tracking, in this mode according the fusion algorithm, the heading vector comes from the IMU sensor and AHRS algorithm, in addition, the displacement is derived by motion sensor. Finally, the fusion algorithm combines them and plot the 3D trajectory.

Figure 11(a) & (b) shows how the capsule is fitted inside the pig's intestine. Considering the 3 cm × 3 cm capsule side, it still fits inside the small intestine. In order to move the capsule freely by hand, the capsule is placed on the intestine, then experiments are performed, as depicted in Figure 11(c). Several paths are created by the intestine and estimated trajectory is calculated.

(a) (b) (c)

Figure 11. Test setup with Pig's intestine.

In Figure 12, three test paths are demonstrated. At each experiment, four plot categories are reported. I) Raw data from IMU sensor. II) Cumulative displacement data from side wall motion camera which denoted as traveled distance. III) The orientation estimation plot from AHRS algorithm which is the result of IMU data fusion. IV) The 3D traveled trajectory which is given by fusion algorithm as described in equation 6.

Finally, the 3D trajectory plot is the fused output of all sensors. In this plot, the dashed line shows the ground truth and blue line shows the estimated trajectory from the proposed algorithm. According to the results, the proposed method could estimate all curves paths correctly. As a result, the overall shape of the traveled path is correctly can be estimated. But, the shape and size of the trajectory matched with the reference track. Another important factor is that the capsule works as long as the sensor surface touches the GI wall; however, the GI tract consists of tubular paths including intestine and esophagus, as well as open areas. In open areas, such as stomach, the capsule tracking may result in errors.

An article by Kalantar-Zadeh, *et al*. [16], analyzed the gas mixtures of different organs in GI, and showed that gas sensing could be a promising method to localize the capsule. So, integrating an Oxygen molecule (O_2) gas sensor to the capsule, could be an option to detect the entrance to the small intestine in the future.

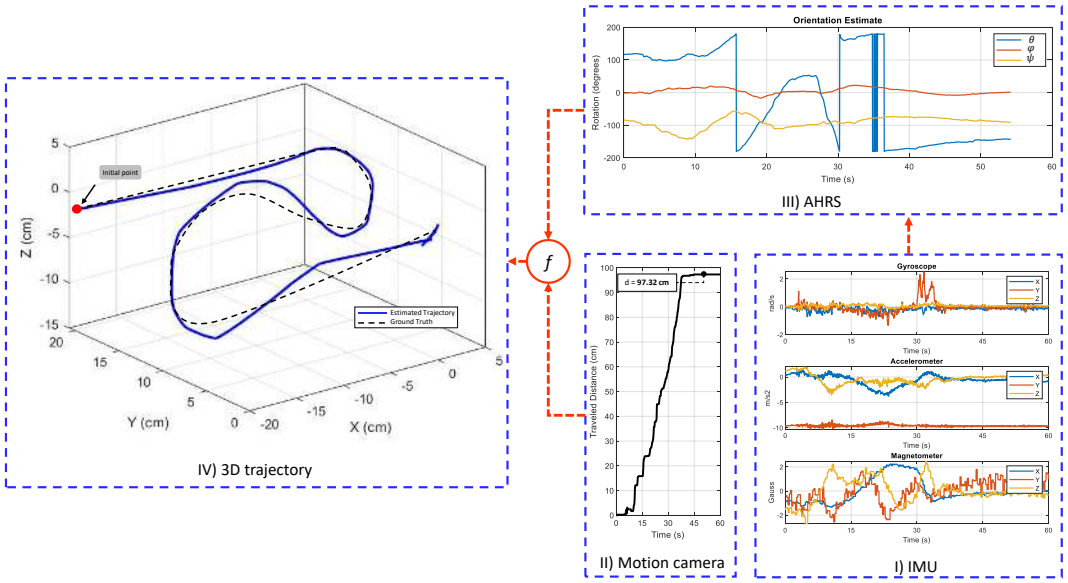

(**a**)

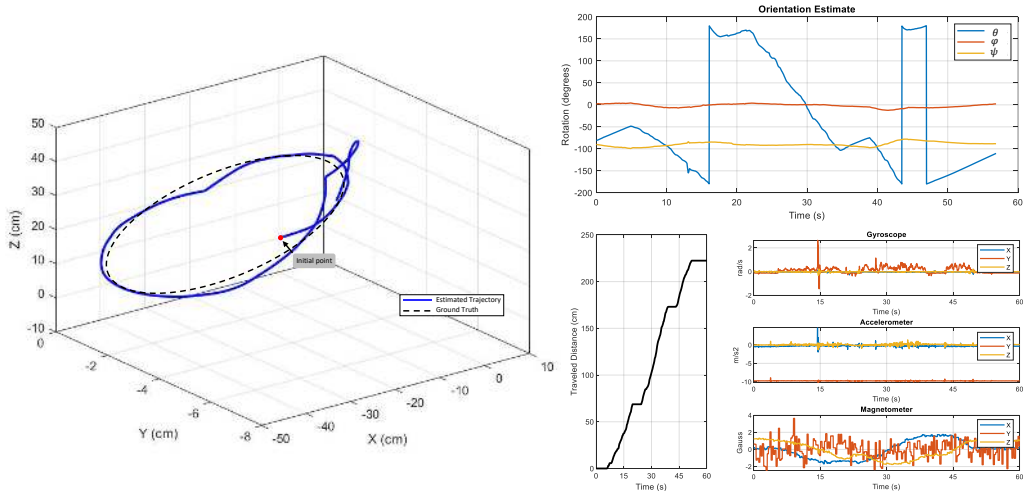

(**b**)

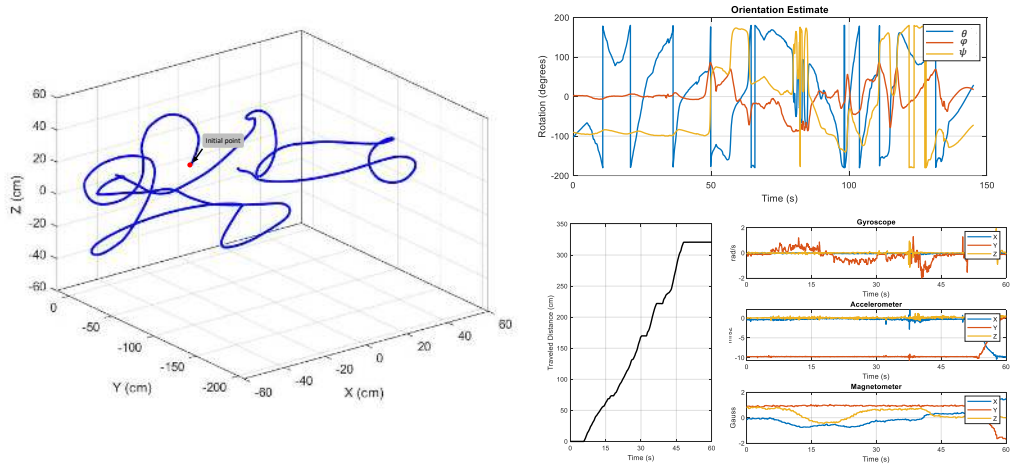

(**c**)

Figure 12. 3D test trajectories (**a**) spiral path, (**b**) oval path & (**c**) random path. The (**a**) is subdivided to, I) raw data from IMU sensor, II) raw data from side wall motion camera, III) orientation estimation [AHRS filter is applied on IMU data to derive the orientation estimation], and IV) computed 3D trajectory [a fusion algorithm merged the orientation estimation and the displacement measured by side wall motion camera to plot the 3D trajectory]. (b) and (c) follows the same format.

Power measurement

Due to the small size of capsule, there is limited space remained for batteries. The battery's capacity is limited, and it must power up the device throughout the process which takes around 8 hours. At this section, the power consumption of the capsule is investigated. Table 2 presents the operating voltage and current in active mode for the device at 3.3 V.

Component	Current (mA)	Power Consumption (mW)
MPU9250	1.84	6.07
ATmega32	1.23	4.06
Red LED	1.28	4.22
Lora	5.25	17.32
Motion sensor	2.10	6.93
Total	**11.70**	**38.61**

Table 2. Estimate of power consumption

In order to work properly for 8 hours, the capsule needs battery with 94 mAh capacity. However, by integrating all the required components in an integrated chip (IC) or a system-on-a-chip (SoC) will lower the power consumption significantly than individual components.

Table 3 provides a list for several intra-body capsule localization methods and compares them based accuracy (how much the estimated measurement is close to the ground truth), extra hardware or weight inside capsule, patient's comfort (i.e., patients' mobility during the period of diagnosis), static reference point (patient's outside movement vs capsule's inside movement), interference of transmitted signal with other sources, involuntary GI motion, and prototype validation (in vitro or in vivo).

The proposed method has several significant advantages. Hospital facility and technician are not required in this method, and it does not confine patient's movement. Most importantly, both patient's external movement and the small bowel's involuntary movement will not interfere with the capsule's internal movement, and the actual displacement of the capsule can be projected. This is because the involuntary motion is rejected by the side wall motion cameras which measure the displacement while the capsule is moving inside the intestine and eliminate the GI motion inside the body. This is something is missing in all other previous works.

Finally, the proposed method is experimentally validated in vitro. However, there are still rooms for improvement and future research is directed towards further improving the WCE localization by improving the sensors and integrating more sensors like, pH and gas sensors.

Conclusion

In this paper we have developed a new method for WCE localization by incorporating an IMU sensor and four side wall motion cameras. The IMU sensor has gyroscope, accelerometer and magnetometer. The data from these sensors are fused together with the aim of AHRS algorithm to estimate the orientation of the capsule. The side wall cameras are similar to an optical mouse sensor which has 18×18 pixels CCD and image processing part in a same chipset. By utilizing a four-camera topology ensures that at least one of them will be in constant touch of the GI wall, and measure the true displacement. Finally, the fusion algorithm combines both orientation and displacement to generate the 3D trajectory. The proposed device has no external reference point. Therefore, comparing with other capsule localization methods this system has many robust features including no interference due to patient's external voluntary movement and small bowel's involuntary internal movements.

Localization Method		Accuracy	Additional hardware inside the capsule	Additional hardware for patients (Patient's comfort)	Static position for reference	Interference	Considering GI involuntary motion	In vitro or in vivo validation	Ref
RF	ToA, Received Signal Strength Indicator (RSSI)	0.2 cm	NO – all necessary modules for RF localization is already implemented in capsules	Extra hardware (antenna array mounted on a cube) must carried by the patients. Limits the patient's mobility significantly	YES- An array of antennas or a belt is required. Antennas must have fixed positions.	Different tissues and muscles lead to inhomogeneous path loss and huge error in localization	Involuntary motion makes GI organs move inside body coordinate while the outside antenna cube is stationary. Results in large error in localization since the RF method is not able to distinguish between these two motions.	NO	[14]
	DoA	1 cm						NO	[7]
	ToA/RSS and Spatial Sparsity	0.8 cm						NO	[15]
Image-based	Hybrid video motion tracking & RF	2.3 cm	NO- The frames captured by the capsule are used for localization	No interference with the patient's mobility	NO- There is no internal reference used to measure the accurate displacement	Fluctuation or inappropriate light. Poor quality imaging, low frames rate causes error in displacement measurement	Image-based localization is partially immune to peristalsis or involuntary motions, but over time, more errors from the missing frames are introduced	YES- The dataset from Pillcam	[16]
	RCNN	3.5 cm						YES- Invitro validation	[17]
Ultrasound imaging	Ultrasonic and MRI	0.2 cm	NO- The capsule is implemented with MRI and ultrasound friendly materials	Performed at hospital by laying on a bed. In addition, a doctor or technician is required to be present all times.	YES- All distances are measured based on sensors' position. Hence, it is considered as a fixed reference for localization	Ultrasound's speed in different materials is the basis of displacement. But it varies in different organs and different human bodies which may cause errors.	The GI organs are visible using this method; hence, we could compensate for the peristalsis motion.	NO	[18]
Radiation imaging	MRI compatible	0.3 cm	NO- The capsule is implemented with MRI friendly materials. Capsule fabrication is expensive.	Performed at hospital by laying on a bed. In addition, a doctor or technician is required to be present all times. Risk of exposing to radiation	YES- The position is measured in coordinates of the MRI device	The electronic devices are not allowed because they cause problems with MRI devices and introduce noises. High level of radiation	The GI organs are visible using this method; hence, we could compensate for the peristalsis motion.	NO	[19]
Magnetic	On-board magnetic sensing	0.5 cm	YES- A small magnet is installed inside the capsule.	An array of hall sensors is attached to the body which limits the patient's mobility significantly	YES- An array of hall sensors is required. Antennas must have fixed positions.	Interference with other sources of magnets. Such as ferromagnetic materials, wires with high current, etc.	Involuntary motion of the GI system inside the body leads to loss of the track of the capsule. Similar issues like RF methods	NO	[20]
	Jacobian-based iterative algorithm	0.7 cm						NO	[21]
	Magnetic sensing	0.5 cm						YES- In vivo validation on a pig	[22]
Proposed method	IMU sensor and sidewall motion cameras	0.95 cm	YES- Sidewall motion camera and IMU sensor.	No additional hardware required. No interference with the patient's mobility.	NO- Track from beginning to the end of GI path with no fixed reference point.	External magnetic field may affect the IMU sensor.	Involuntary and peristalsis motions have no interference with the actual motion	YES- In vitro validation on pig intestine	

Table 3. Comparing available WCE localization methods

References

1. Iddan, G., Meron, G., Glukhovsky, A. & Swain, P. Wireless capsule endoscopy. *Nat.* **405**, 417, DOI: https://doi.org/10.1038/35013140 (2000).
2. *Medtronic, Smartpill.* https://www.medtronic.com/covidien/en-ca/products/motility-testing/smartpill-motility-testing-system.html.
3. Alam, M. W., Vedaei, S. S. & Wahid, K. A. A Fluorescence-Based Wireless Capsule Endoscopy System for Detecting Colorectal Cancer," *Cancers (Basel)* **12**, 890, DOI: https://doi.org/10.3390/cancers12040890 (2020).
4. Khan, A. H., Sohag, M. H. A., Vedaei, S. S., Mohebbian, M. R. & Wahid, K. A. Automatic Detection of Intestinal Bleeding using an Optical Sensor for Wireless Capsule Endoscopy. *In 42nd Annual International Conference of the IEEE Engineering in Medicine & Biology Society (EMBC),* 4345–4348, DOI: https://doi.org/10.1109/EMBC44109.2020.9176340 (2020).
5. Deeba, F., Bui, F. M. & Wahid, K. A. Computer-aided polyp detection based on image enhancement and saliency-based selection. *Biomed. Signal Process. Control* **55**, 101530, DOI: https://doi.org/10.1016/j.bspc.2019.04.007 (2020).
6. Nafchi, A. R., Goh, S. T. & Zekavat, S. A. R. Circular arrays and inertial measurement unit for DOA/TOA/TDOA-based endoscopy capsule localization: Performance and complexity investigation, *IEEE Sens. J.* **14**, 3791–3799, DOI: https://doi.org/10.1109/JSEN.2014.2331244 (2014).
7. Goh, S. T., Zekavat, S. A. R. & Pahlavan, K. DOA-based endoscopy capsule localization and orientation estimation via unscented kalman filter. *IEEE Sens. J.* **14**, 3819–3829, DOI: https://doi.org/10.1109/JSEN.2014.2342720 (2014).
8. Ciuti, G., Menciassi, A. & Dario, P. Capsule endoscopy: from current achievements to open challenges. *IEEE Rev. Biomed. Eng.* **4**, 59–72, DOI: https://doi.org/10.1109/RBME.2011.2171182 (2011).
9. Hany, U. & Wahid, K. A. An adaptive linearized method for localizing video endoscopic capsule using weighted Centroid algorithm. *Int. J. Distrib. Sens. Networks* **2015**, DOI: https://doi.org/10.1155/2015/342428 (2015).
10. Khan, U., Ye, Y., Aisha, A. U., Swar, P. & Pahlavan, K. Precision of em Simulation Based Wireless Location Estimation in Multi-Sensor Capsule Endoscopy. *IEEE J. Transl. Eng. Heal. Med.* **6**, DOI: https://doi.org/10.1109/JTEHM.2018.2818177 (2018).
11. Wang, M., Shi, Q., Song, S., Hu, C. & Meng, M. Q. H. A novel relative position estimation method for capsule robot moving in gastrointestinal tract. *Sensors (Basel)* **19**, 2746, DOI: https://doi.org/10.3390/s19122746 (2019).
12. Taddese, A. Z., Slawinski, P. R., Pirotta, M., De Momi, E., Obstein, K. L. & Valdastri, P. Enhanced real-time pose estimation for closed-loop robotic manipulation of magnetically actuated capsule endoscopes. *Int. J. Rob. Res.* 37, 890–911, DOI: https://doi.org/10.1177/0278364918779132 (2018).
13. Shao, G., Tang, Y., Tang, L., Dai, Q. & Guo, Y. X. A Novel Passive Magnetic Localization Wearable System for Wireless Capsule Endoscopy. *IEEE Sens. J.* **19**, 3462–3472, DOI: https://doi.org/10.1109/JSEN.2019.2894386 (2019).
14. Ito, T., Anzai, D. & Wang, J. Novel joint TOA/RSSI-based WCE location tracking method without prior knowledge of biological human body tissues. in *36th Annual International Conference of the IEEE Engineering in Medicine and Biology Society (EMBC)*, 6993–6996, DOI: https://doi.org/10.1109/EMBC.2014.6945237 (2014).
15. Pourhomayoun, M., Jin, Z. & Fowler, M. L. Accurate localization of in-body medical implants based on spatial sparsity. *IEEE Trans. Biomed. Eng.* **61**, 590–597, DOI: https://doi.org/10.1109/TBME.2013.2284271 (2014).
16. Bao, G., Pahlavan, K. & Mi, L. Hybrid Localization of Microrobotic Endoscopic Capsule Inside Small Intestine by Data Fusion of Vision and RF Sensors. *IEEE Sens. J.* **15**, 2669–2678, DOI: https://doi.org/10.1109/JSEN.2014.2367495 (2015).
17. Turan, M., Almalioglu, Y., Araujo, H., Konukoglu, E. & Sitti, M. Deep EndoVO: A recurrent convolutional neural network (RCNN) based visual odometry approach for endoscopic capsule robots. *Neurocomputing* **275**, 1861–1870, DOI: https://doi.org/10.1016/j.neucom.2017.10.014 (2018).
18. Pagoulatos, N., Edwards, W. S., Haynor, D. R. & Kim, Y. Interactive 3-D registration of ultrasound and magnetic resonance images based on a magnetic position sensor. *IEEE Trans. Inf. Technol. Biomed.* **3**, 278–288, DOI: https://doi.org/10.1109/4233.809172 (1999).
19. Krieger, A. *et al.* An MRI-compatible robotic system with hybrid tracking for MRI-guided prostate intervention. *IEEE Trans. Biomed. Eng.***58**, 3049–3060, DOI: https://doi.org/10.1109/TBME.2011.2134096 (2011).
20. Salerno, M. *et al.* A discrete-time localization method for capsule endoscopy based on on-board magnetic sensing. *Meas. Sci. Technol.* **23**, 015701, DOI: https://doi.org/10.1088/0957-0233/23/1/015701 (2012).
21. Di Natali, C., Beccani, M., Simaan, N. & Valdastri, P. Jacobian-Based Iterative Method for Magnetic Localization in Robotic Capsule Endoscopy. *IEEE Trans. Robot.* **32**, 327–338, DOI: https://doi.org/10.1109/TRO.2016.2522433 (2016).
22. Pham, D. M. & Aziz, S. M. A real-time localization system for an endoscopic capsule using magnetic sensors. *Sensors (Basel)* **14**, 20910–20929, DOI: https://doi.org/10.3390/s141120910 (2014).
23. Lee, H. C., Jung, C. W. & Kim, H. C. Real-time endoscopic image orientation correction system using an accelerometer and gyrosensor. *PLoS One* **12**, DOI: https://doi.org/10.1371/journal.pone.0186691 (2017).
24. Kalantar-Zadeh, K. *et al.* A human pilot trial of ingestible electronic capsules capable of sensing different gases in the gut. *Nat. Electron.* **1**, 79–87, DOI: https://doi.org/10.1038/s41928-017-0004-x (2018).
25. Jang, J. *et al.* A four-camera VGA-resolution capsule endoscope system with 80-Mb/s body channel communication transceiver and sub-centimeter range capsule localization. *IEEE J. Solid-State Circuits* **54**, 538–549, DOI: https://doi.org/10.1109/JSSC.2018.2873630 (2019).

Acknowledgements

This paper is funded by Federal New Frontiers in Research Fund (NFRF).

Author contributions statement

S.S.V. designed and implemented the electronic circuitries of the system and drafting the paper as well as do the in-vivo tests, and acquisition, analysis, and interpretation of the results. K.A.W is the supervisor and provided a secure fund for the project. He also comprehensively edited and revised the paper.

Competing interests

The authors declare no competing interests.

Figures

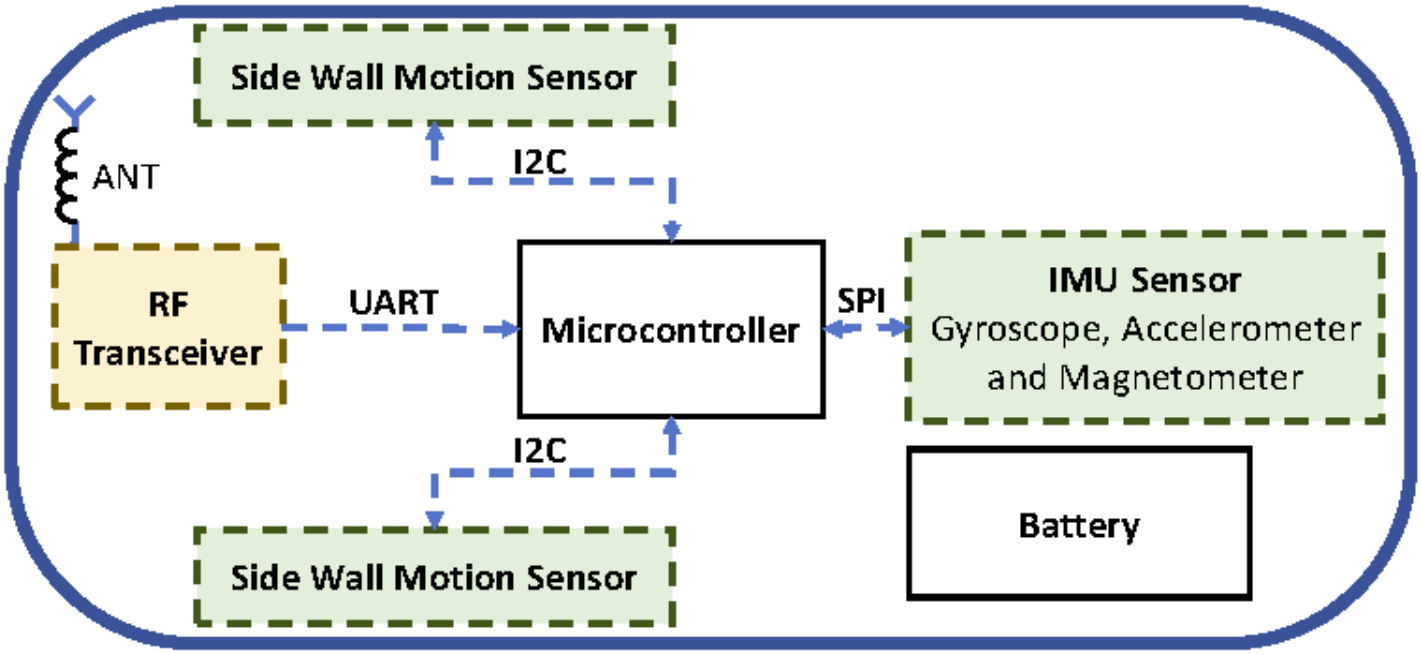

Figure 1

Schematic overview of the capsule.

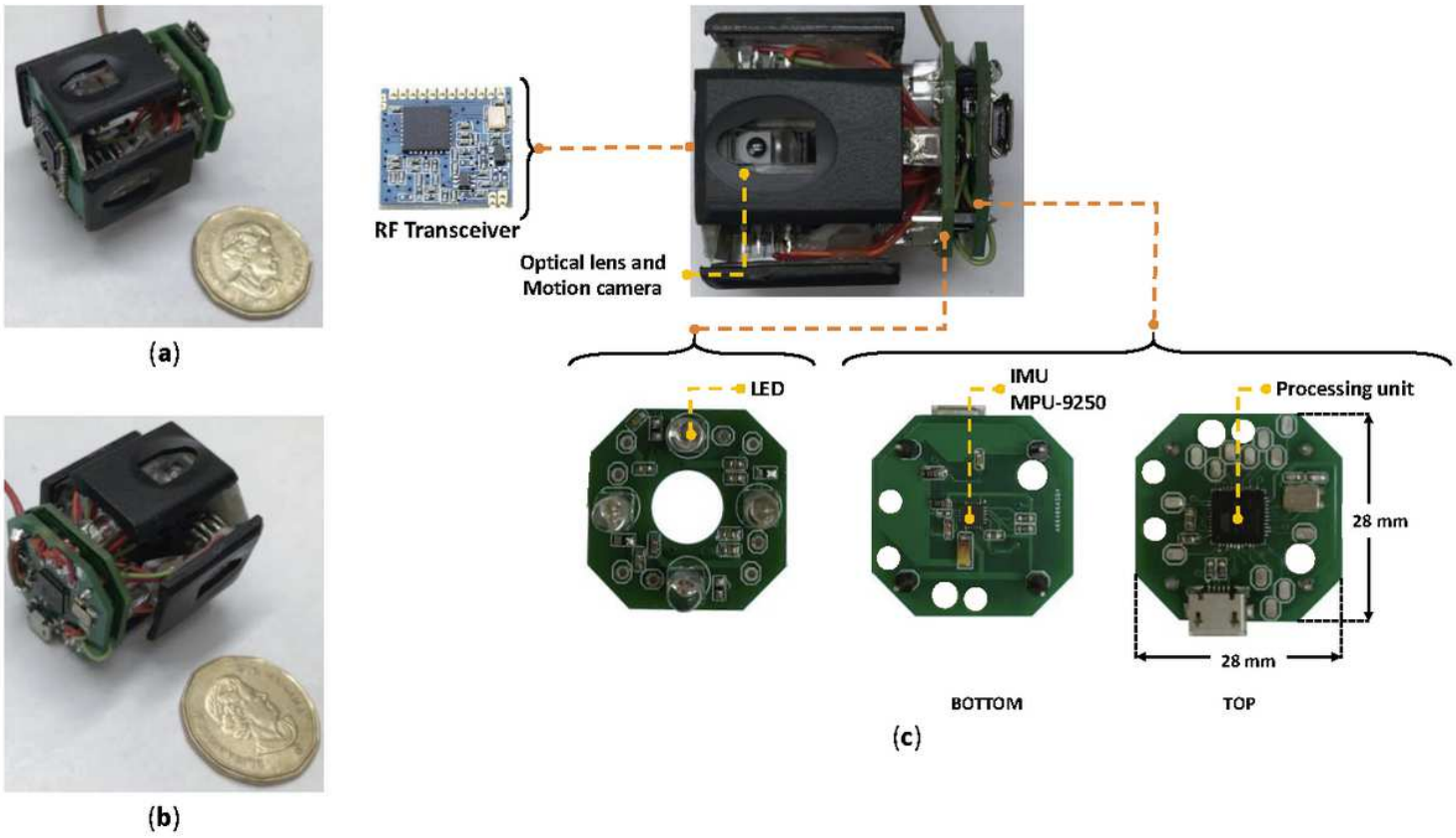

Figure 2

(a) & (b) Capsule prototype designed in the lab (c) Various parts of the lab prototype.

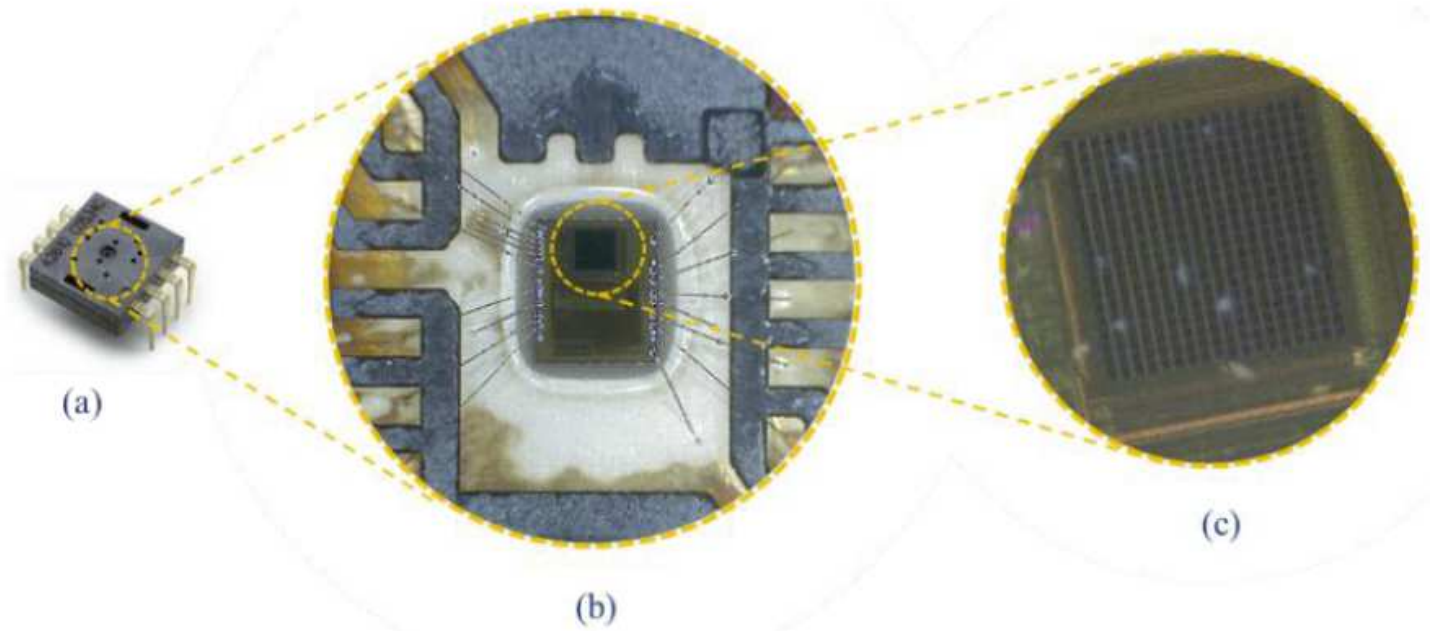

Figure 3

Optical motion measurement sensor (similar to the one used in computer optical mouse today), (a) Dual inline package IC, (b) Microscopic view and (c) 18×18 pixels CMOS camera.

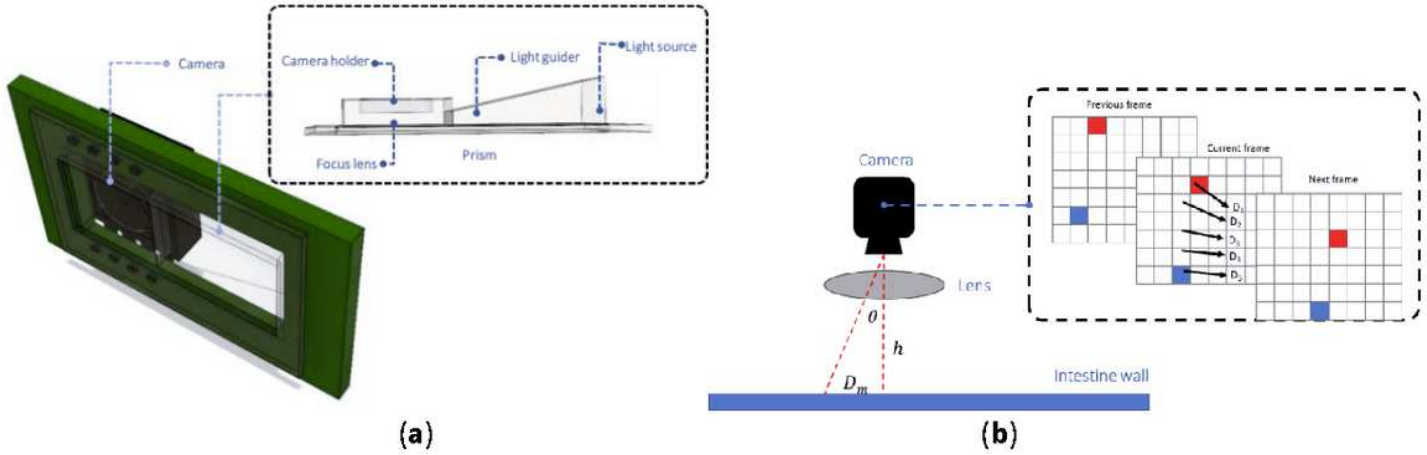

Figure 4

(a) Side wall camera and its optical parts, (b) motion vector calculation.

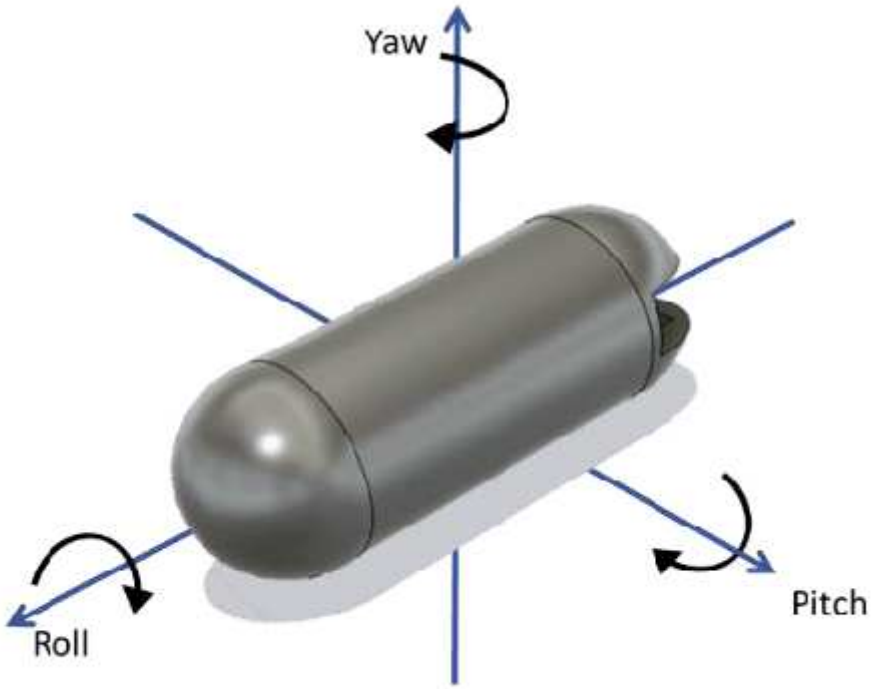

Figure 5

rotation about different axes.

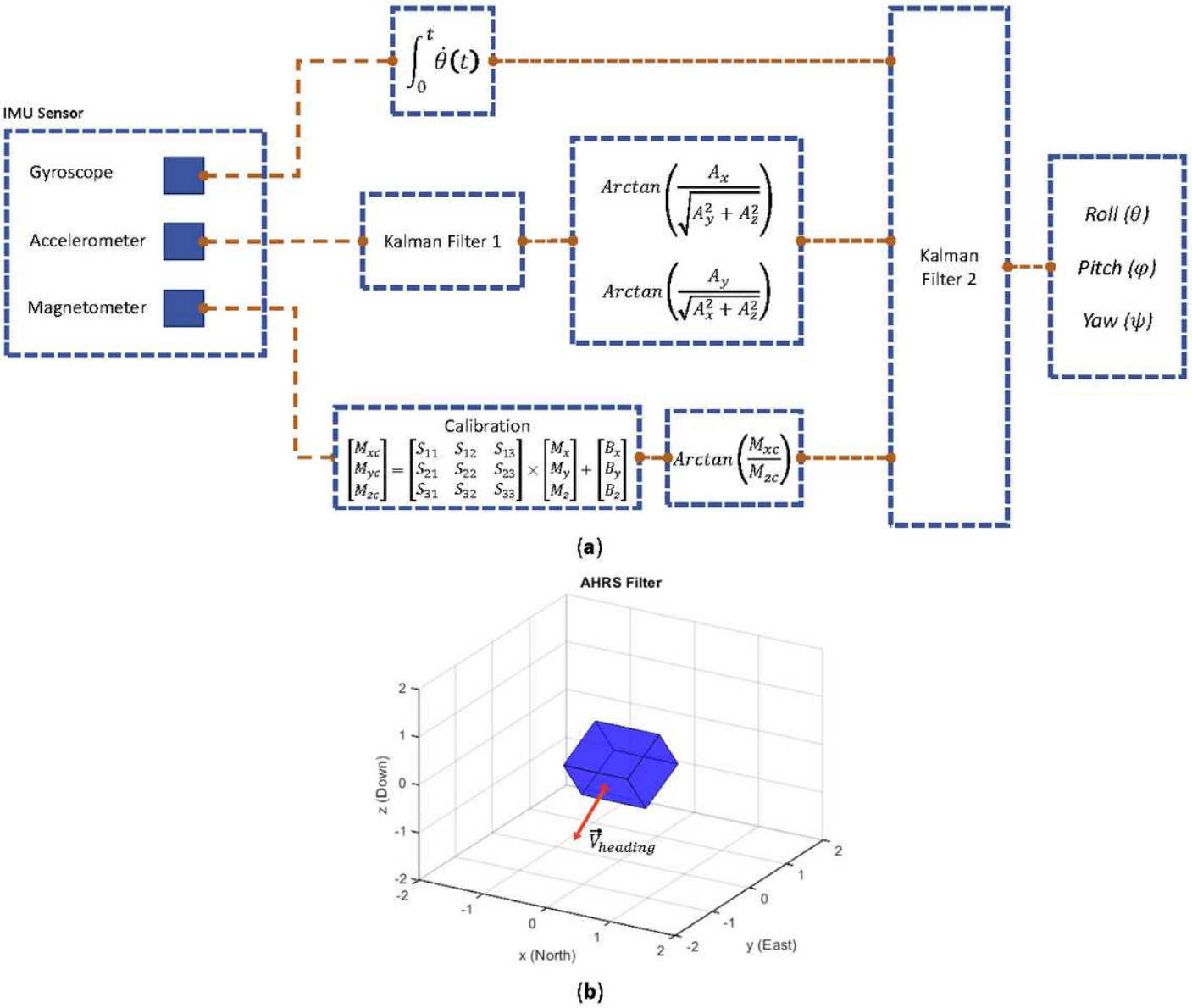

Figure 6

(a) IMU sensor fusing schematic, (b) 3D orientation result.

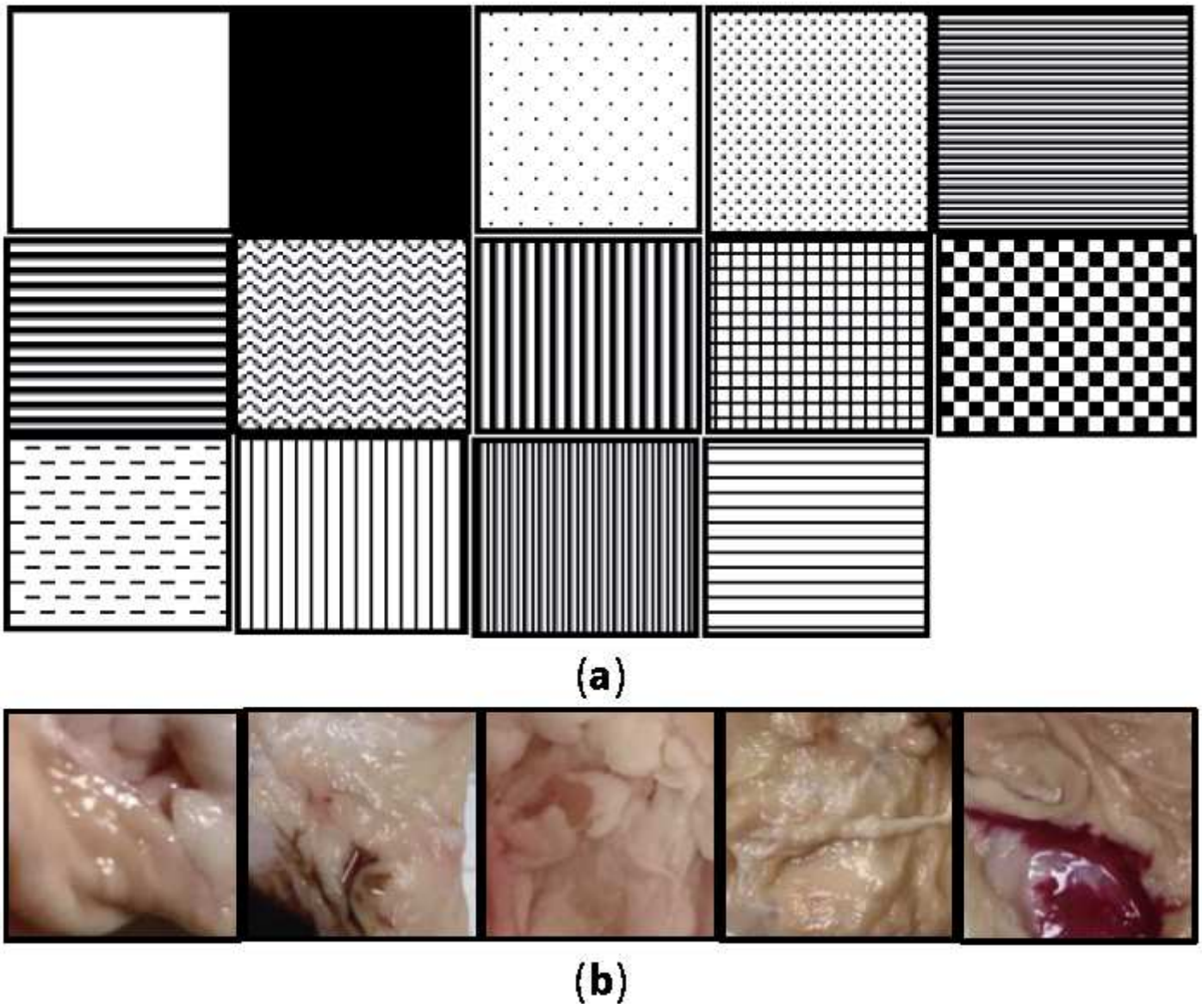

Figure 7

(a) Basic patterns, (b) colored patterns.

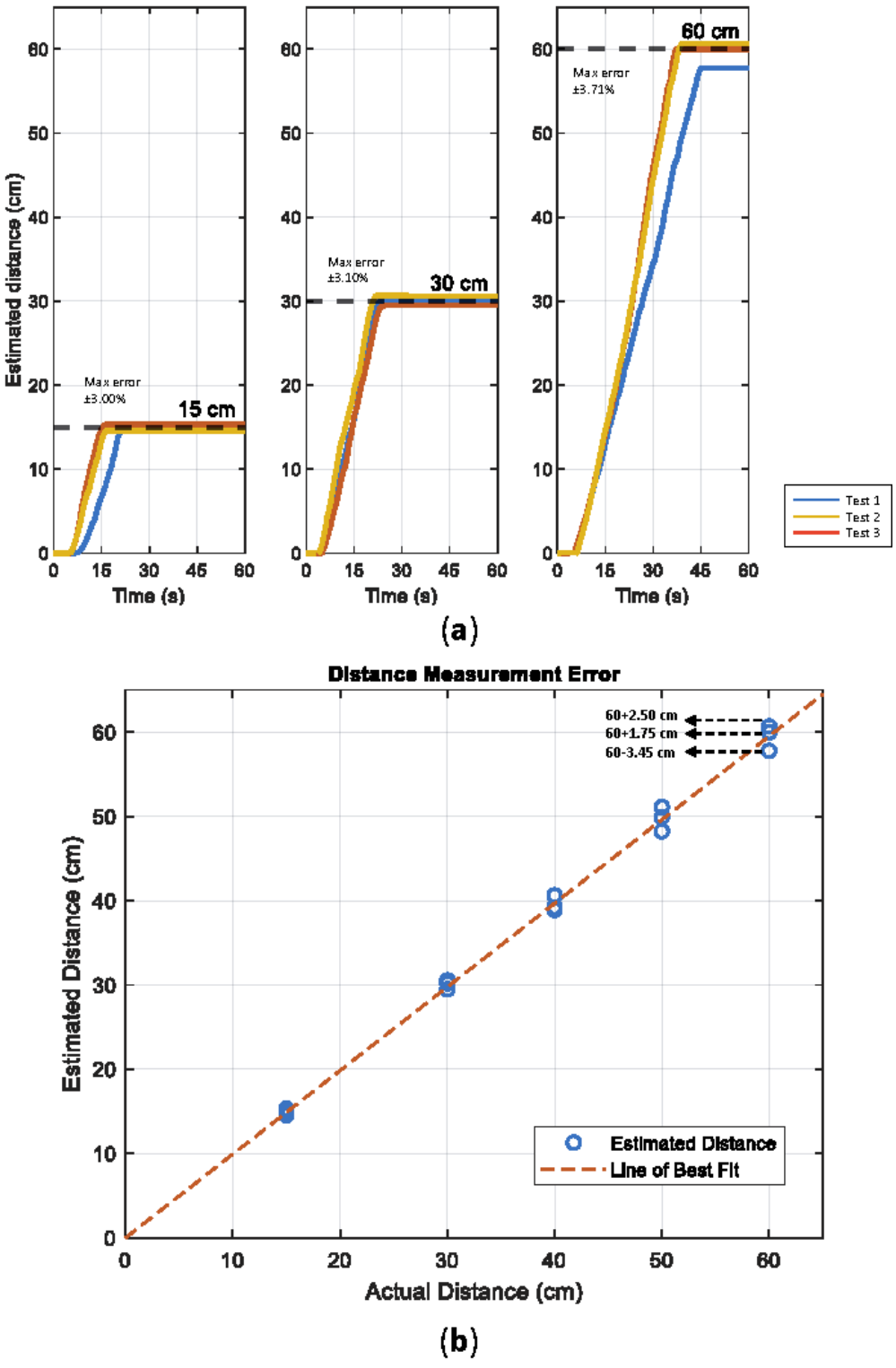

Figure 8

(a) Repeat the same path (b) Distance measurement error.

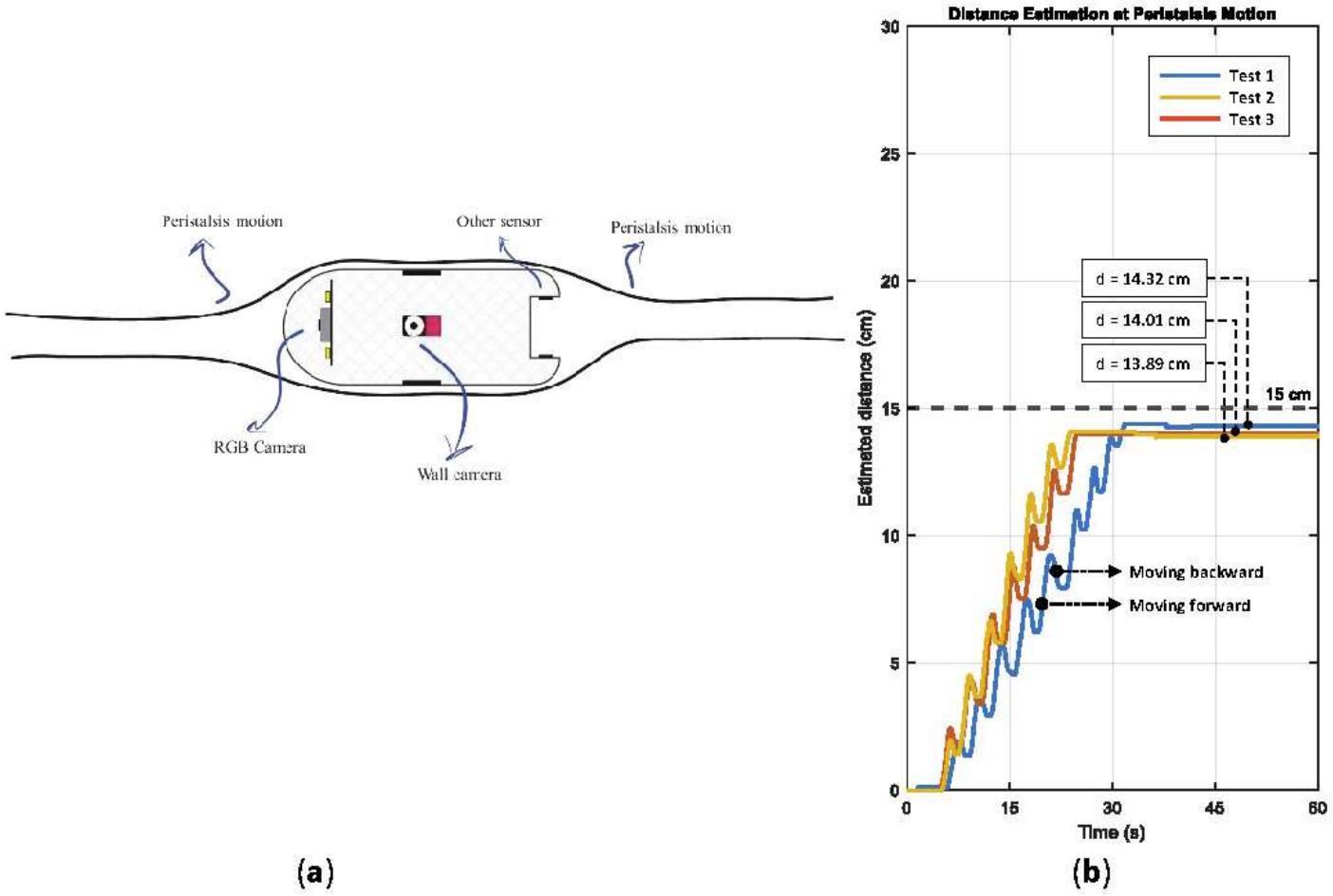

Figure 9

(a) Peristalsis motion (b) experiment results.

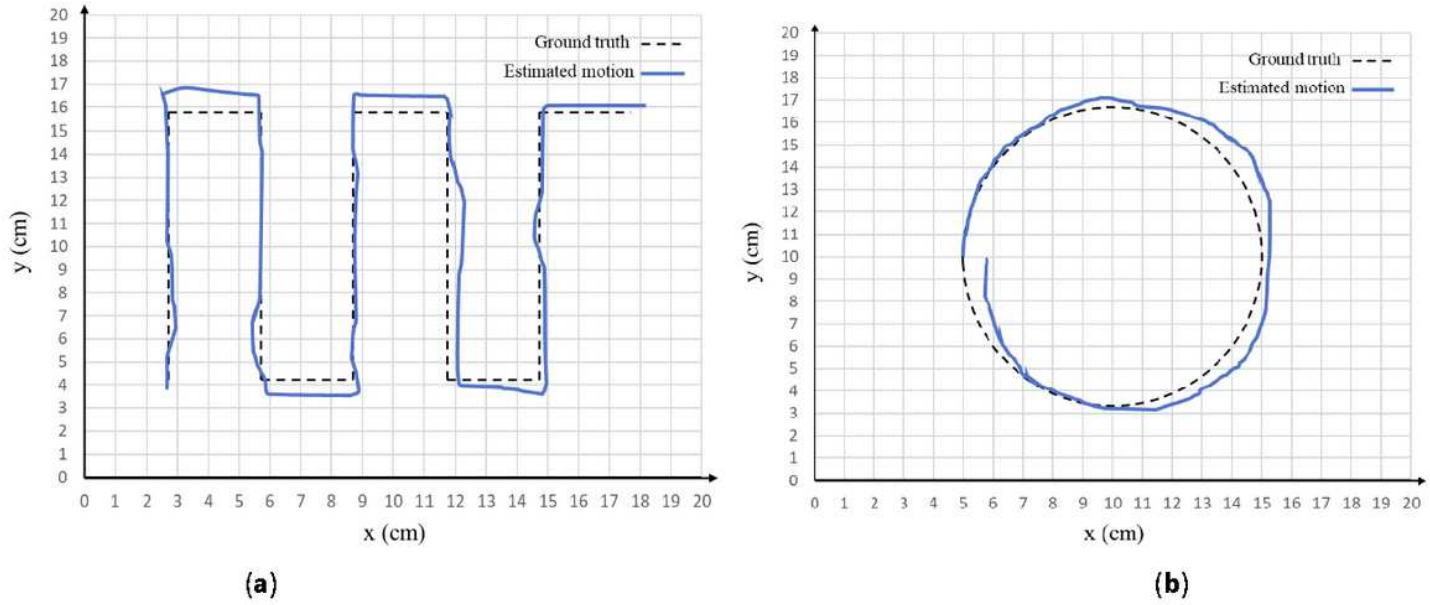

Figure 10

2D motion tracking, (a) & (b) test trajectories.

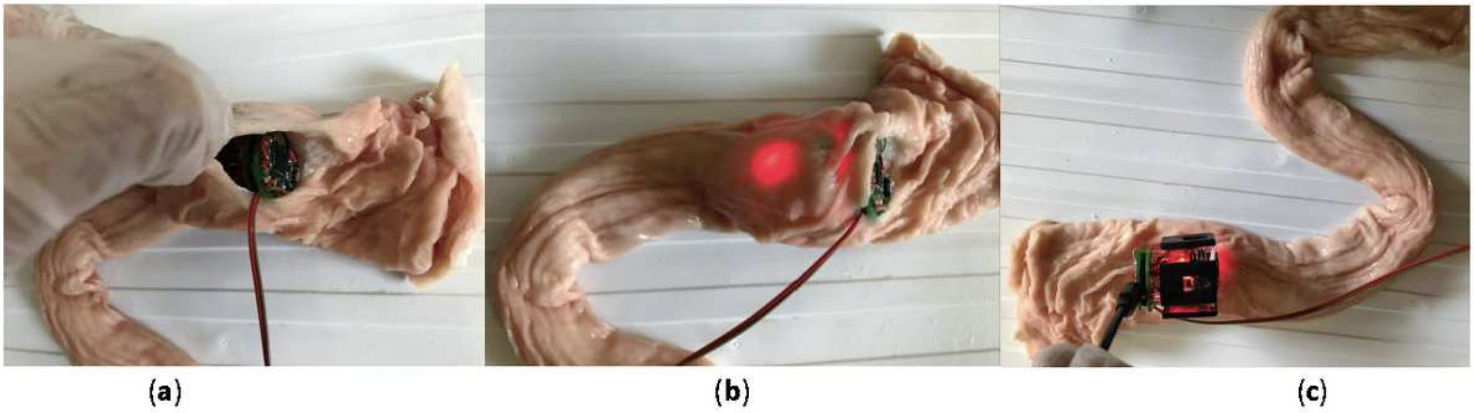

Figure 11

Test setup with Pig’s intestine.

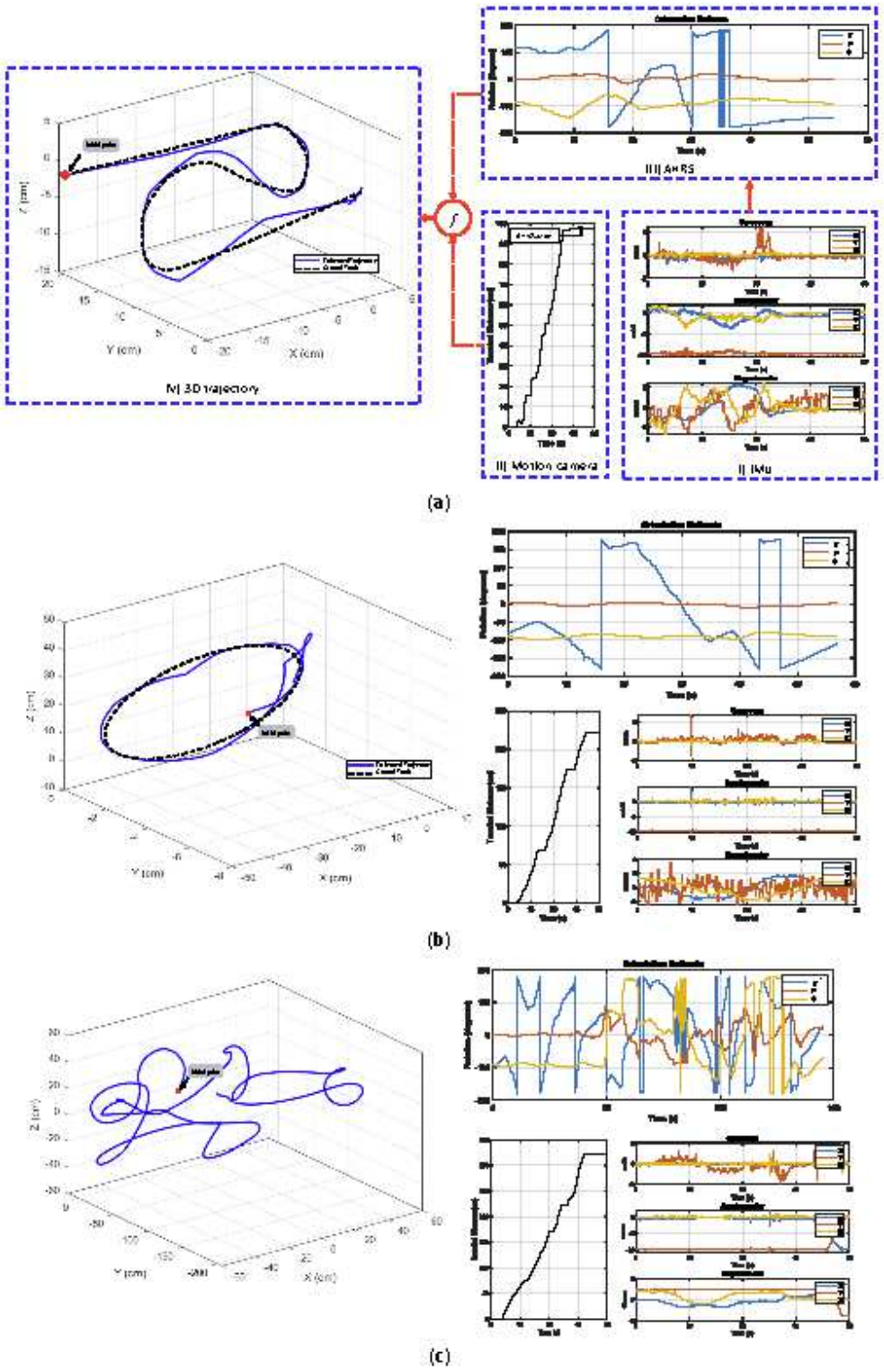

Figure 12

3D test trajectories (a) spiral path, (b) oval path & (c) random path. The (a) is subdivided to, I) raw data from IMU sensor, II) raw data from side wall motion camera, III) orientation estimation [AHRS filter is applied on IMU data to derive the orientation estimation], and IV) computed 3D trajectory [a fusion algorithm merged the orientation estimation and the displacement measured by side wall motion camera to plot the 3D trajectory]. (b) and (c) follows the same format.